proceedings

Sixth Annual Symposium

incremental motion control systems and devices

Professor B.C. Kuo, Editor

may 24 – 27, 1977

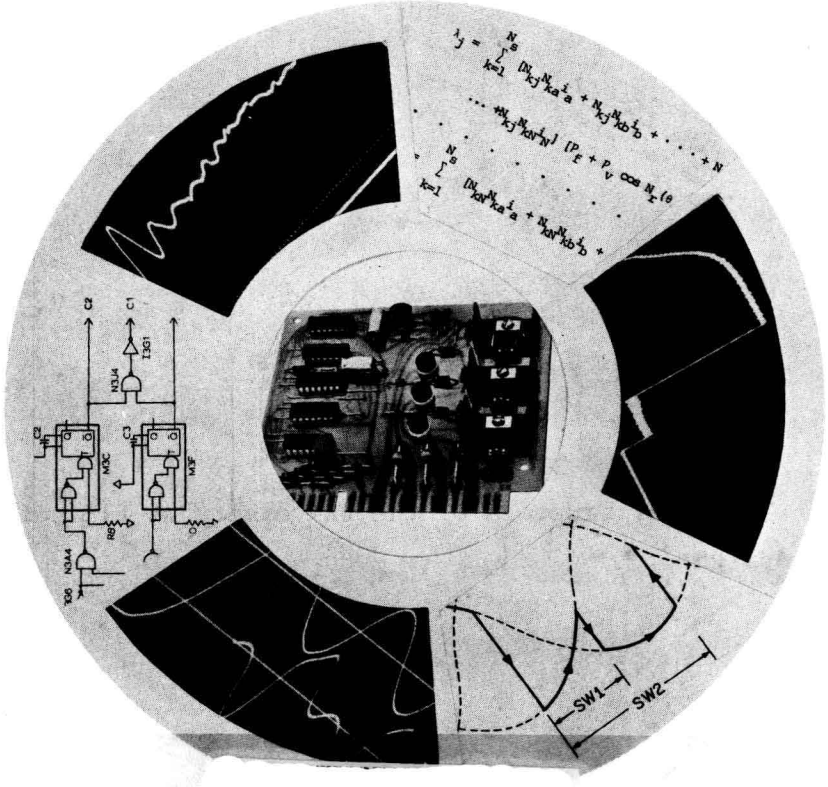

Department of Electrical Engineering
University of Illinois at Urbana-Champaign

in cooperation with

Warner Electric Brake and Clutch Company, Beloit, Wisconsin

and

Westool Ltd., Durham, England

All rights reserved. No part of this book may be reproduced in any form or by any means without permission in writing from Prof. Benjamin C. Kuo.

© 1977 by the Board of Trustees of the University of Illinois at Urbana-Champaign

Printed by Braun & Brumfield Inc., Ann Arbor, Michigan.

Price: 35 dollars.

FOREWARD

The Sixth Annual Symposium on Incremental Motion Control Systems and Devices was held at the University of Illinois at Urbana-Champaign on May 24-27, 1977. The Symposium was cosponsored by the Electrical Engineering Department of the University of Illinois at Urbana-Champaign; the Warner Electric Brake and Clutch Company, Beloit, Wisconsin; and Westool Limited, Durham, England. These Proceedings contain the papers presented at the Symposium.

At this Symposium, which has been held on an annual basis since 1972, technological information and new ideas were interchanged. The technical papers encompassed a broad area on motion control problems, and many represented original contributions of research and development carried out by leading universities and companies. A record number of papers were accepted at the 1977 Symposium.

The support of the College of Engineering, Department of Electrical Engineering; Warner Electric Brake and Clutch Company; and Westool Limited is acknowledged. The encouragement of Dr. E. C. Jordan, Head of the Department of Electrical Engineering; Dr. O. L. Gaddy and Dr. E. W. Ernst, Associate Heads of the Department of Electrical Engineering; and Mr. W. W. Keefer, President, Warner Electric Brake and Clutch Company, is greatly appreciated.

The editor is grateful to Bill Arrott and Bob Schmidt of Gardner, Jones and Company, Inc., Chicago, for providing pre- and post-symposium publicity, and to Jane Carlton for her assistance in many aspects of the preparation of the Symposium and of the manuscripts for these Proceedings. Special thanks are due to Mrs. Lilian Beck, editor of the Publications Office of the Electrical Engineering Department who provided valuable editorial assistance, and to the rest of the publications staff for their assistance. Thanks are also due to Harold B. Lawler and Rosa Townsend for their handling of the financial aspects of the Symposium.

B. C. Kuo
May 1977

TABLE OF CONTENTS

此为试读,需要完整PDF请访问: www.ertongbook.com

IMPROVED DAMPING FOR STEP MOTORS

Kenneth S. Kordik

Warner Electric Brake and Clutch Co.
Beloit, Wisconsin

I. INTRODUCTION

A step motor has an inherent characteristic which causes it to overshoot when taking a step. This is because in the one-phase-on excitation mode, there is no retarding or stopping torque exerted on the rotor to stop it until the rotor moves past its detent position. Various schemes have been proposed which reduce the rate of current decay in the switched-off phase. While this has a positive effect on the overshoot of the motor, the time required to transit a step is greatly increased and the dynamic torque and speed of the motor are reduced.

Step motors can be operated with two phases energized at one time. This greatly reduces the overshoot and oscillations. In a four-phase motor both static and dynamic torques are increased at the expense of additional power and heating in the motor. In order to move or step from one position to another, one phase is turned off and the next phase is turned on. If the motor is being operated with two phases energized at one time, a phase remains energized for two steps. If a motor is stepped from C and D phases on to D and A phases on, D phase remains energized. The current in C phase decays while the current in phase A builds up. The rotor begins to move to the new detent position. As the rotor begins to move, the inductances of the phases change. The inductance of phase C decreases while the inductance of phase D increases, until the rotor has reached a position one half way between the old and new positions, at which point the inductance of phase D begins to decrease and the inductance of phase A begins to increase as the rotor moves to the new detent position. However, since the inductance and the flux decrease with increasing current, (the motor is an iron-core device) the net inductance will depend on the rotor velocity. The velocity also effects the counter EMF, which effects the current in the windings. The result is that the net torque exerted on the rotor varies and tends to reduce the overshoot and the oscillations. This is the reason that a step motor with two phases energized overshoots and oscillates less. With one phase on there is less interaction between the windings.

In the standard motor this type of damping scheme is not adequate for most applications. Damping can be improved by increasing the number of turns in the motor to increase the counter EMF and to increase the flux density.

II. A STEP MOTOR WITH IMPROVED DAMPING

Another way to improve damping is to add a fixed source of flux which increases the flux and counter EMF and reduces the inductance of the windings, thus permitting faster current rise, which increases the rotor velocity, thus resulting in greater counter EMF. With two phases energized, adjacent poles of the opposite polarity are energized, resulting in flux leakage. Magnetic devices always exhibit some flux leakage. When two poles of opposite polarity are in close proximity to each other, the flux leakage can be substantial. It depends on the reluctance of the flux path. In a step motor, the leakage flux varies with rotor position.

Placing magnets between poles results in less leakage, thus more torque is developed by the motor. Figure 1 shows the schematic diagram of a new step motor with permanent magnets placed between the stator poles. The result of this invention is that the motor has more holding torque, develops some static torque, (so it stays in position with the power off), the single-step transit time is reduced, the overshoot and oscillations are reduced, and the dynamic torque is improved.

Figure 2 shows a comparison between the responses of the motor with magnets and the same motor without the magnets when driven with the same control and power supply. Identical windings are used in both motors.

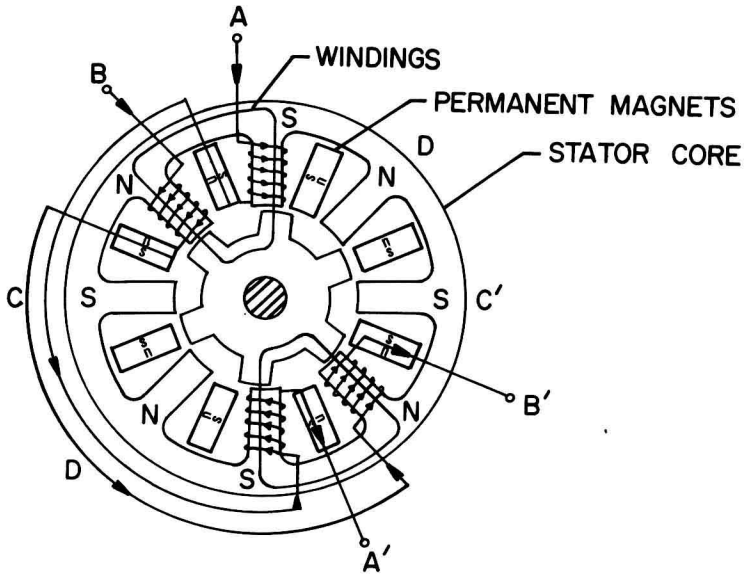

Figure 1. Cross-section diagram of a four-phase, variable-reluctance step motor with permanent magnets between stator poles. Only the A and B phase windings are shown.

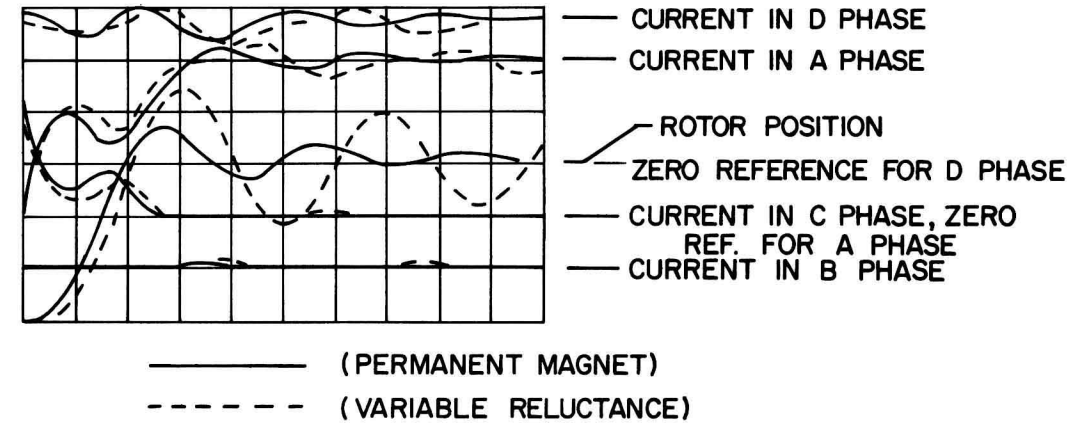

CALIBRATION/DIVISION			
	HOR.	2 msec.	
	VERT.	5°	0.5 AMP.

Figure 2. Single-step response from CD phase to DA phase with 0.000164 oz-in-sec^2 inertia load. Two phases on, 24 volts at 1.6 A per phase, 8.6 ohm in series with each phase. 8 ohm resistor diode suppression.

Since the magnetic circuit is partially saturated due to the permanent magnet flux, current and flux rise faster. This causes the rotor to begin moving sooner and at a higher rate. This results in increased counter EMF in the phase which has been turned on. Part of the increased EMF is due to the permanent magnets. This causes the current to dip to less than 1/2 the normal value. The dip occurs just as the rotor approaches the detent position. The net result is that D phase exerts increased torque on the rotor which slows down the rotor and tends to stop it. At the same time, the current in phase D is increasing back to a normal value. This is reached just as the rotor goes beyond its normal detent position. Without the permanent magnets, the current in D phase does not peak out until the rotor is well beyond the normal detent position, thus making the torque produced less effective in stopping the rotor.

As the rotor overshoots and comes back to the detent position, the current in phase A peaks and phase D current is reduced. This causes a retarding torque on the rotor, while the motor without magnets has a minimum current in phase D as the rotor crosses the detent position, but the current in phase A lags behind; thus, it is less effective in stopping the rotor oscillations. Phase C also tries to hold the rotor back. Phase C current is higher in the PM version motor than in the VR version.

Current changes in the turned-off phase are also losses which tend to reduce or damp out the oscillations. The current change in the PM motor is higher than that of the VR motor.

Table I lists the inductance values of the two motors. The inductance of the PM motor is less than half that of the standard motor with no DC excitation. This difference is reduced as DC current is applied to the windings.

TABLE I.

DC Bias Current	Inductance, Millihenries	
	Permanent Magnet	Variable Reluctance
0 Amps D.C.	12.81	26.14
0.5 Amps D.C.	15.42	24.33

Table II lists the torque values acting on the rotor as the motor moves through various positions while executing a single-step motion.

TABLE II.

Dynamic Torque at Various Rotor Positions During a Single-Step Motion.

Voltage 24
Phases On 2
Current 1.6 Amps/Phase
Control 8.6 Ohm Current Limiting Resistors in Series with Each Phase
Suppression 8 Ohm Resistor Diode
Load: Inertia 16.4×10^{-3} oz-in-sec.^{2}
Friction None
Rotor Inertia 12.0×10^{-3} oz-in-sec.^{2}

Rotor Position, Degrees	Remarks	Torque Oz.-In.	
		PM Motor	VR Motor
0	Initial detent position	0	0
0	Start		-0.05
1		6.0	8.6
3		19.0	17.0
5		18.0	16.1
7		12.0	12.0
9		1.0	5.5
11.3		-5.5	2.1
15	Final detent position	-7.0	-3.8
17	Overshoot	-12.2	-9.9
18.5	Overshoot	-12.0	-14.0
15	Detent position	6.2	1.0

These values are based on the current values in the various windings at the various rotor positions. Negative torques will slow the rotor down and tend to stop it, while positive values of torque cause it to accelerate. This occurs until the motor reaches the detent position. At this point, the rotor slows down until it stops and reverses direction. After the rotor reverses direction, positive torques tend to stop it until it reverses direction again.

Table II clearly shows why the permanent-magnet motor overshoots less and damps out quicker. As the rotor approaches the final detent position, the negative torque tends to brake the rotor to a stop, while in the variable-reluctance motor the

torque is low; it, nevertheless, causes the rotor to continue to accelerate until it reaches the detent position. Note that the PM motor has higher torque in the positive or forward direction after the rotor returns to the detent position. The rotor is rotating backwards; therefore, the positive torque is actually stopping it. Referring to Figure 2 will clarify this point.

This motor is covered by U.S. Patent No. 3,984,711.

此为试读,需要完整PDF请访问: www.ertongbook.com

ADAPTIVE STEP MOTOR DAMPING USING CURRENT FEEDBACK

J. D. Unger

Motorola Inc.
Arlington Heights, Illinois

I. INTRODUCTION

Adaptive damping is a technique for providing optimum damping for a stepping motor over a range of loads which would cause oscillation in a standard constant-parameter damping system. The standard damping scheme outputs a damping signal (or signals) to the step motor controller after a fixed delay from the time the motor reaches the next-to-last step of its excursion. The delay is adjusted when the system is installed so that the nominal motor load will be damped with little or no oscillation. If the load on the motor changes due to wear, or over the normal range of travel of a mechanism, the nonadaptive system may become oscillatory. The adaptive system can detect load changes on the motor at the time of damping and adjust the damping time delays to yield oscillation-free damping. The usefulness of such a system depends on how much the system load changes and on how much oscillation can be tolerated.

Basically, the adaptive damping system treated here consists of using parameters in the current waveforms of variable-reluctance step motors to determine the damping delays needed for optimum damping. The position of peaks in the current waveforms and the magnitude of the current change as the load on the motor changes. These parameters are measured as the motor is accelerating or decelerating in the damping process.

The basics of damping and of closed-loop control are omitted from this paper for brevity but can be found in references [2]-[5].

II. OBSERVING THE MOTOR CURRENTS

We wish to observe the currents in each of the motor phases. Two schemes were tried. The first, shown in Fig. 1, is the simplest.

The voltage across R_s is proportional to the current in whichever phase is energized. By observing V_s, the "on-current" in each phase is observed one at a time. The value of R_s is such

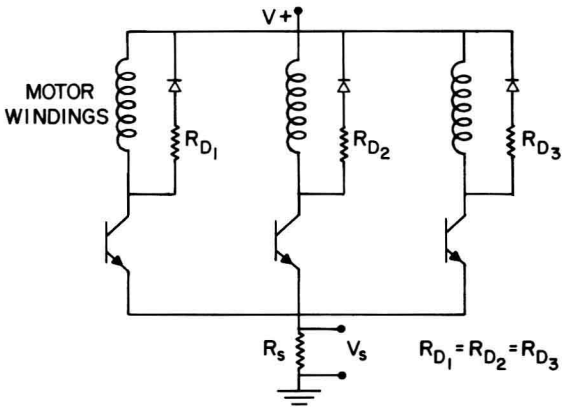

Figure 1. Common-phase current sensing.

that the maximum voltage drop across it is a few tenths of a volt. This allows the circuitry controlling the driver transistors to operate properly. The resistors R_{D_1} - R_{D_3} are suppression resistors. A large value of R_D will allow the current in the winding to decay more rapidly when its driver transistor is turned off, but it subjects the transistor to a higher flyback voltage.

The second current-sensing scheme is shown in Fig. 2. It provides measurements of both the on-currents and the off-currents of each phase separately.

The resistors R_D serve the same purpose as before. The three sensing resistors R_{s1}, R_{s2}, R_{s3} have equal values, small in comparison to the phase winding resistance. The resistor R_B is a bias resistor, which prevents the current in any phase from ever reaching zero exactly. Its value is large in relation to the winding resistance. The diodes D_1, D_2, D_3 isolate the phases, allowing one bias resistor to be used for all three phases. The need for the bias resistor is to prevent clipping of the current waveforms.

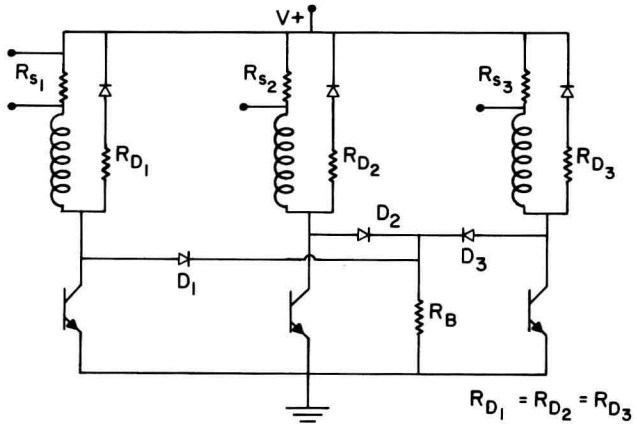

Figure 2. Three-phase current sensing.

The motor used for most of the following tests was a Warner Electric SM024-0035-AA three-phase variable-reluctance step motor. The maximum holding torque of the motor is rated at 35 oz-in; the winding resistance is 20Ω, and the recommended supply voltage is 28 volts. To one end of the motor shaft is connected a MCS 1600-2 dual optical encoder and a continuous-rotation potentiometer with negligible friction and inertia. The other end of the shaft is coupled to a Vibrac TQ-100 torque transducer. Coupled to the torque transducer is either a variable inertial load or a variable frictional load. The frictional load consisted of an aluminum disk with an inertia of about three to four times rotor inertia and two pressure pads of adjustable compression. This device was found to give sufficiently repeatable measurements of friction. Friction measurements were made by running the motor at a constant speed and observing the torque. The setup is shown in Fig. 3.

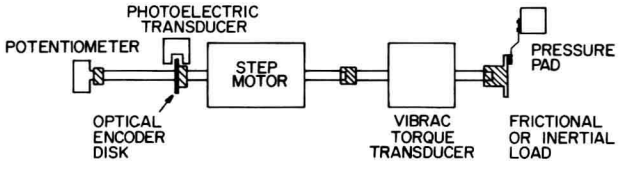

Figure 3. Mechanical setup.

The electrical setup is shown in block diagram form in Fig. 4. The Warner driver card requires TTL level pulses to make the phases switch in a continuous clockwise or counterclockwise sequence. The torque transducer is connected directly to a meter supplied with it. The optical encoder provides a "glich-free" TTL output with one rising and one falling edge per motor step.

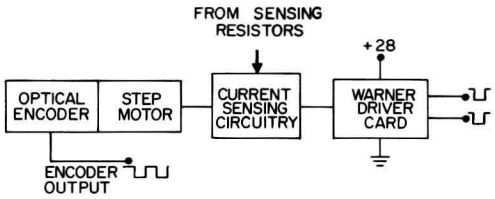

Figure 4. Electrical setup for running and testing.

III. CORRELATION BETWEEN MAGNITUDE OF CURRENT WAVEFORMS AND DAMPING CHARACTERISTICS

A block diagram of the desired damping system is shown in Fig. 5. The only input to the damping controller is a signal from the logic that runs the motor to tell when to begin the damping process, and the current waveforms of the motor. All the

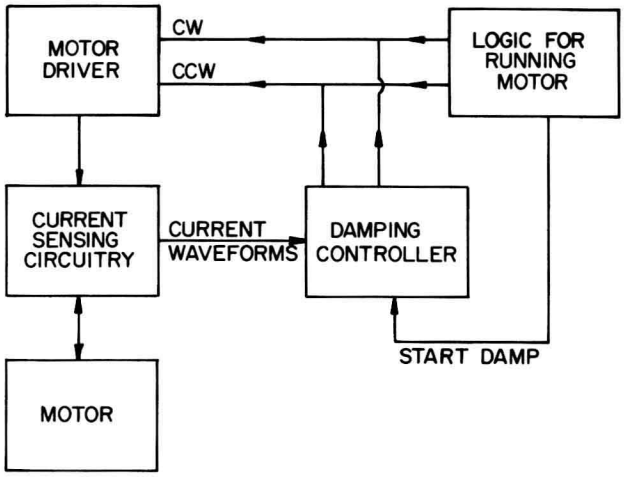

Figure 5. Desired damping system.

information needed to choose the correct damping times - friction, inertia, and speed of the motor - must be transmitted to the controller through the current waveforms.

The simplest case to begin observations of the current waveforms is the single-step case. Two initial conditions are known: the initial speed is zero and the initial position is phase A detent. If the motor is at rest at phase A with that phase energized, and the power is switched to phase B, the waveforms in Fig. 6 are produced. If instead of just energizing phase B, we energize B at $t = 0$, then energize A at $t = t_1$, and phase B again at $t = t_2$, then by varying t_1 and t_2 we can obtain a perfectly damped single-step response. Typical waveforms produced by switching at t_1 and t_2 to get perfect damping are shown in Fig. 7. These are obtained from the circuit in Fig. 2, with $R_D = 0$, $R_{s1} = R_{s2} = R_{s3} = 0.07\Omega$, and $R_B = 100\Omega$.

It was decided to measure the voltages at fixed times across the sensing resistors and then to obtain a correlation between the magnitudes of these voltages and the two unknown damping parameters t_1 and t_2. Figure 8 shows the results for various loads.

Figure 8 shows the voltage measured across the sensing resistor of phase A, which is denoted by $V_a(3)$, versus t_1, starting at $t_1 = 3$ milliseconds. Note that t_1 is the time at which phase A is deenergized and phase B energized.

Let $V_a(0.5)$ denote the voltage measured across R_{s1}, the sensing resistor of phase A, starting at 0.5 msec after $t = t_1$. Figure 8(b) shows the relation between the magnitude of $V_a(0.5)$ and $t_2 - t_1$, which represents the time duration between turning B off and turning A on again. Figure 8(c) shows the voltage $V_b(0.5)$ which was measured under the same condition as described above but across the sensing resistor of phase B. The actual value of the load used is not shown; however, the smallest time t_1 corresponds to the load consisting of the potentiometer and the optical encoder disk only, and the largest time t_1 corresponds to a load of 6.2 times rotor inertia. Only inertial loads were used in this experiment.

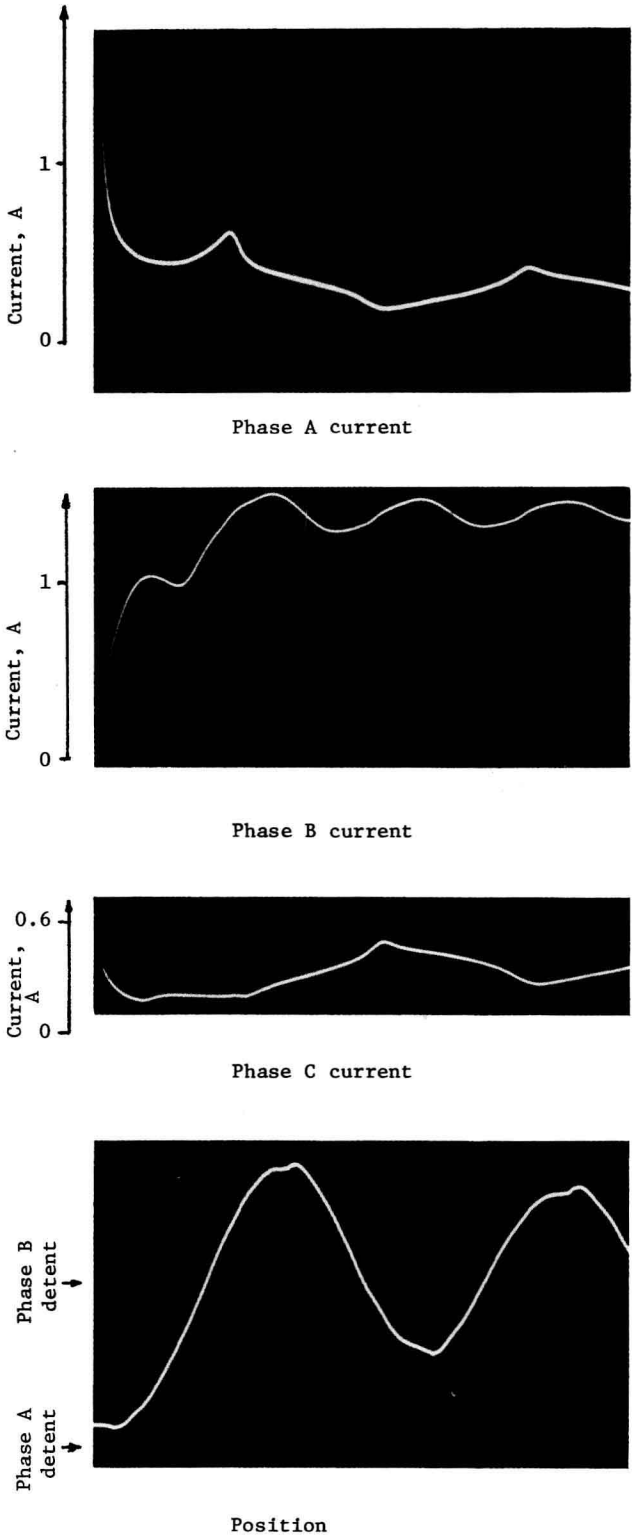

Figure 6. Single-step response and current waveforms.

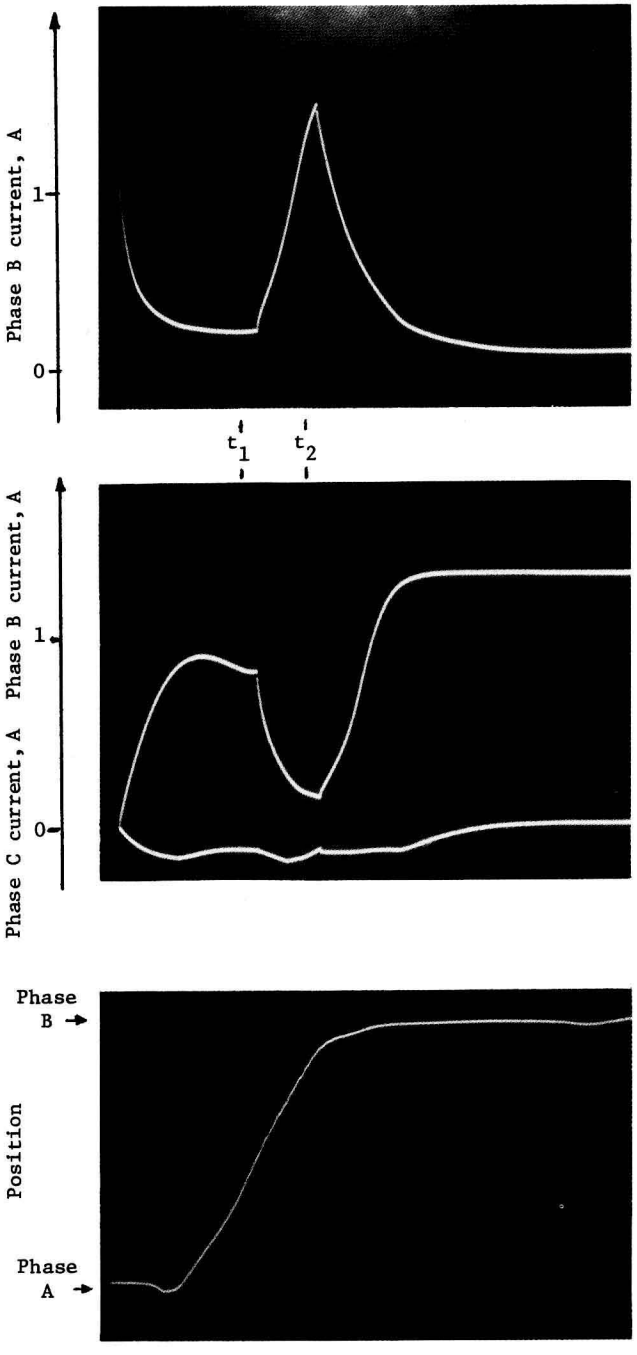

Figure 7. Damped single-step response and current waveforms.

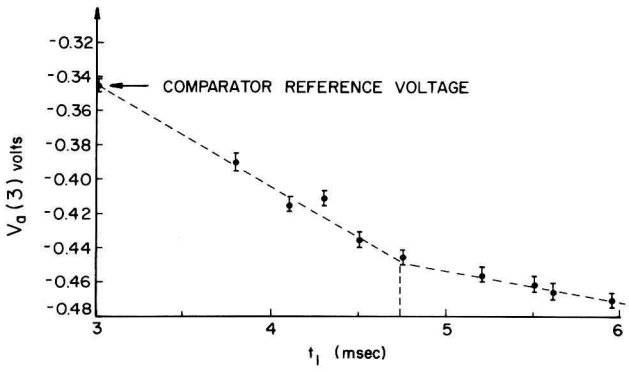

Figure 8(a). Magnitude of phase A current versus t_1 for various loads.

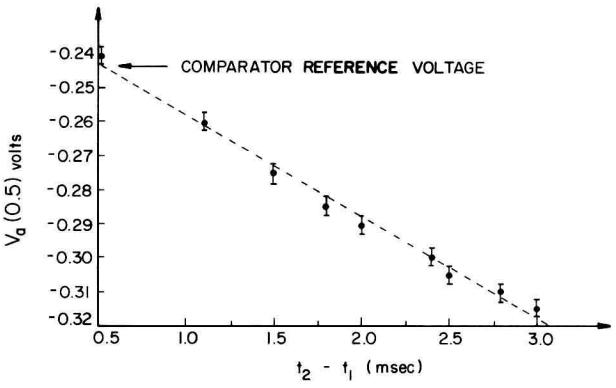

Figure 8(b). Magnitude of phase A current versus $(t_2 - t_1)$ for various loads.

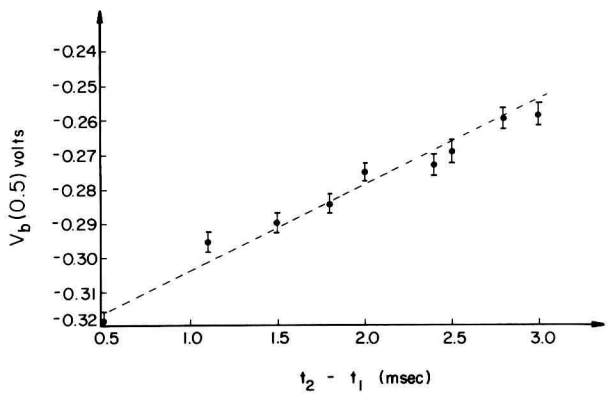

Figure 8(c). Magnitude of phase B current versus $(t_2 - t_1)$ for various loads.

From observation of the graphs in Fig. 8, we see that a linear approximation can be made to the curve in Fig. 8(a) from $t_1 = 3$ to $t_1 = 4.75$. To extend the graph to cover the entire range of loads, a piecewise-linear approximation can be used. This is shown on the graph with a dotted line. The graphs in Figs. 8(b) and 8(c) appear to be linear over the entire range, so a straight line can be used to approximate either one of these.

Since the graphs in Figs. 8(b) and 8(c) are both linear, either could be used to implement a damping scheme. To avoid switching between waveforms, however, only voltages measured from the phase A sensing resistor were used.

IV. DESIGN OF SYSTEM FOR MAGNITUDE DETECTION

To implement a damping scheme using the magnitude of the current waveform, the system shown in Fig. 9 was developed.

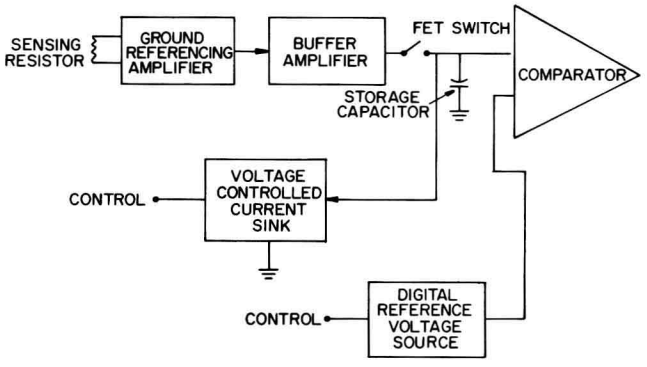

Figure 9. Magnitude-sensing damping scheme.

The Ground-Referencing Amplifier provides unity gain ground referencing of the voltage across the sensing resistor with a low CMRR (common mode rejection ratio). A low CMRR is important to isolate power supply fluctuations from current waveform changes. The buffer amplifier provides a gain and a low impedance to drive the storage capacitor. An FET switch functions like a sample-and-hold.

The first step in the sequence of operation is that the ground-referencing amplifier must be connected to the proper sensing resistor. An analog multiplexer could be used for this purpose. Next, the FET switch closes to sample the waveform for 3 msec. At the end of 3 msec, the switch opens and the voltage-controlled current sink begins to linearly decrease the voltage on the storage capacitor at a rate determined by the slope of the graph in Fig. 8(a). When the voltage on the capacitor reaches a voltage determined by the digital reference voltage source, the comparator changes. The time t_1 has been reached and a pulse is sent to the motor driver to switch to phase A. The FET switch closes again for 0.5 msec, the capacitor voltage is decreased linearly at a rate determined by the graph of Fig. 8(b), and a pulse is sent out to switch the motor to phase B when the voltage across the storage capacitor reaches the voltage of the reference source. This is time t_2. The voltage of the reference source is selected to be the voltage at the vertical intercept of the graph of Fig. 8(a) when making the first comparison, and the voltage at the vertical intercept of the graph of Fig. 8(b) for the last comparison.

The above is a description of a system that makes two voltage-to-time conversions which are strictly linear. To create a piecewise-linear approximation, an additional comparator could be added that would sense the voltage at which the change of slope in the graph of Fig. 8(a) was to occur. The comparator could then modify the voltage-controlled current sink to change the slope appropriately.

V. EVALUATION OF MAGNITUDE DETECTION

The prototype adaptive damper worked well using the laboratory setup. The prototype contained a piecewise-linear approximation scheme as discussed before, which aids in damping large loads. It provided less than 10% of one step overshoot for any inertial load between only the encoder disk and potentiometer, and 6 times rotor inertia. Friction in most cases made overshoot and ringing less. In some cases, the system would overcompensate for the friction and produce an overshoot greater than that without friction, but it was always less than 10%.

There was generally a fair amount of difficulty

in adjusting the parameters of the system. The important user adjustments are the slopes and intercepts of the graphs in Figs. 8(a) and 8(b), the threshold point for the piecewise-linear approximation, and the slope during the piecewise-linear approximation (the right side of the graph of Fig. 8(a)).

An important disadvantage of magnitude sensing is that fluctuations of sensing resistor values and motor winding resistance from one phase to another make the system asymmetrical. Keeping the value of the sensing resistors small will allow high-tolerance, low-wattage resistors to be used, which will help cure this problem.

Other external parameters which will produce errors in the magnitude-sensing scheme are no load power supply voltage fluctuations and changes in motor temperature which change the winding resistance as well as the damping requirements.

VI. CORRELATION OF CURRENT PEAKS AND DAMPING PARAMETERS

Thus far we have discussed the motor when making just one step, and the initial speed and position are known exactly. When the motor has advanced two or more steps and it is desired to stop damped, we can only approximate the speed and position just before damping occurs. When the motor is accelerating or decelerating, the speed is changing constantly and the position is difficult to estimate. The simplest situation occurs when the motor is running at a constant average speed and it is desired to stop damped from that speed.

An experiment was set up where the motor was run closed loop until it reached a constant speed and then stopped at a predetermined rotor position. No damping was used. Figure 10 shows the waveform of the current in phase B when the motor is run closed loop for twenty-two steps and stopped on phase B. While the motor is running, the current cannot build up to its peak value. When the rotor reaches the last step, the current surges upward and then oscillates before settling to its nominal value. This oscillation is due to the oscillation of the rotor around its final position.

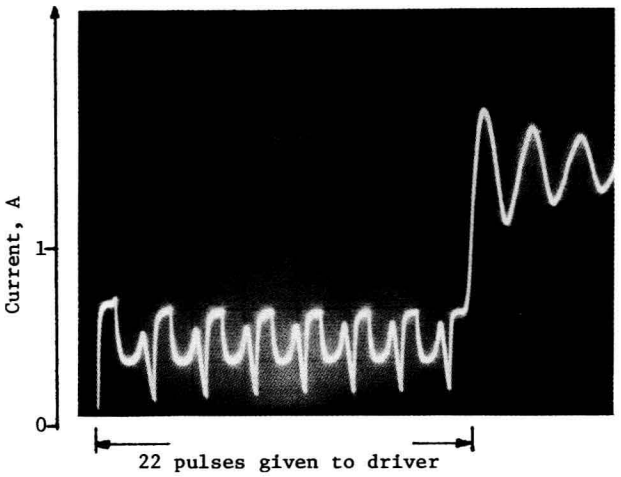

Figure 10. Phase B current versus time, 22 steps.

Figure 10 shows the current waveform of one of the phases for a complete 22-step excursion. At the beginning, the initial velocity is zero and the initial position is known. We could, therefore, make measurements similar to those in the single-step damping scheme described earlier, while the motor is making its first step. This data, which would be a measure of the load on the motor, could be stored until the end of the run when the motor is to be damped. We could then measure the speed of the motor just before damping by measuring the time between the last two pulses sent to the driver. Combining the speed with the information about the load obtained at the beginning of the run and some knowledge of the rotor position, we should have enough information to damp the motor on the 22nd step so that it will stop damped on the 23rd step. The knowledge of rotor position could come from running the motor closed loop and knowing the lead angle of the encoder. The disadvantages of a scheme like this are that we must store the information about the load for an indefinite amount of time, and, if the load changes from the beginning to the end of the run, there will be an error. In practical systems frictional load often changes as a printer head travels from one end to the other of a screw or as lubrication heats up and becomes less viscous. Inertial loads might change as paper is wound off a spool. Storage of analog information for an indefinite amount of time requires conversion of

此为试读,需要完整PDF请访问: www.ertongbook.com